EARTH SURFACE PROCESSES AND LANDFORMS
Earth Surf. Process. Landforms (2018)

Published online in Wiley Online Library
(wileyonlinelibrary.com) DOI: 10.1002/esp.4525

Form-based river restoration decreases wetland hyporheic exchange: Lessons learned from the Upper Colorado River

Matthew S. Sparacino,[1]* Sara L. Rathburn,[1] Timothy P. Covino,[2] Kamini Singha[3] and Michael J. Ronayne[1]
[1] Geosciences, Colorado State University, Fort Collins, Colorado 80523, USA
[2] Ecosystem Science and Sustainability, Colorado State University, Fort Collins, Colorado 80523, USA
[3] Hydrologic Science and Engineering Program, Colarado School of Mines, Golden, Colorado 80401, USA

Received 8 July 2017; Revised 21 September 2018; Accepted 27 September 2018

*Correspondence to: M. S. Sparacino, Colorado State University, Geosciences, 1482 Campus Delivery, Fort Collins, Colorado, 80523, USA. E-mail: sparacino.matt@gmail.com

ESPL
Earth Surface Processes and Landforms

ABSTRACT: Restoration of river–wetland systems to recover lost ecosystem services and restore consistent flood regimes is commonly directed at modifying in-channel storage and hyporheic exchange. Here, we monitored the hydrologic response to channel realignment in a montane river–wetland system by comparing pre- and post-restoration measurements. In 2015, an earthen berm and 190 m segment of the Upper Colorado River were constructed to consolidate flow from multiple channels into the historic thalweg. We injected a sodium chloride tracer during baseflow and used mass-balance calculations and electrical resistivity imaging to assess changes in near-channel hyporheic exchange. Results indicate a decrease in hyporheic exchange within the wetland due to lost complexity along the consolidated flow path. Subsurface complexity appears to control hyporheic exchange more than surface complexity. Flow consolidation increased the area-adjusted wetland water yield by 231 mm, indicating a loss of wetland water storage capacity. One year of post-restoration monitoring suggests that the form-based channel restoration directed at consolidating flow into a single thread adversely affected the hyporheic exchange functioning in the pre-restoration system. Results from this case study are applicable to restoration planners as they consider the effects of form-based projects on water storage capacity in similar systems. © 2018 John Wiley & Sons, Ltd.

KEYWORDS: river restoration; wetland restoration; hyporheic exchange; electrical resistivity; tracer test

Introduction

River and wetland restoration have become increasingly popular in the United States in response to ecosystem degradation (Bernhardt and Palmer, 2011). Total wetland area in the continental United States has decreased by more than half during the past 200 years as a result of human activities and land use changes, especially due to water diversions, farming, and urbanization (Dahl, 2000; Cooper *et al.*, 2012). Climate change threatens to further degrade river-wetland systems as precipitation, flow conditions, and temperature become more unpredictable (Erwin, 2009). Freshwater wetlands, which are the largest wetland type in the United States, are most susceptible to losses (Dahl, 2000). Forested and shrub freshwater wetlands are common in the intermountain west where relict glacial topography, abundant precipitation, and cool temperatures support their growth (Cooper *et al.*, 2012). When functioning properly, surface water–groundwater exchange in river-wetland complexes facilitates valuable ecosystem services, including water filtration and nutrient cycling (Triska *et al.*, 1989; Zedler and Kercher, 2005). When paired with overbank flooding, these processes allow wetlands to support diverse ecological communities (Junk *et al.*, 1989). Common river-wetland restoration goals aim to recover specific ecosystem services and restore consistent flood regimes, but quantitative evaluations of restoration outcomes are often lacking (Bernhardt and Palmer, 2011). If restoration is to remain effective at offsetting wetland losses, targeted monitoring is essential to assess how well restoration practices achieve specific project goals.

Historically, river restoration has prioritized the enhancement of form over function (Wohl *et al.*, 2015). The benefits of form-based restoration are often short-lived, and restoration practitioners have recently adopted a more holistic and process-based approach with broadened goals that incorporate ecological, geomorphological and aesthetic components (Palmer *et al.*, 2005). Many river forms do not persist without a sustaining process; therefore geomorphic processes are directly connected to essential ecological functions that rely on them. For example, small-scale bed form modifications were commonly used to improve fish habitat and water quality in attempts to reverse degradation caused by centuries of navigation-focused river management (Gowan and Fausch, 1996; Wohl *et al.*, 2015). But this attention to river form, which is often limited to the channel reach scale, is not sustainable unless additional factors needed to support such bed

modifications, like channel slope, substrate grain size, and land use changes, are also addressed. In other cases, single-thread sinusoidal meander bends were imposed on rivers to support fish habitat (Newbury, 1995), even in reaches where coarse bed sediments did not naturally support this channel form. Alternatively, restoration aimed at increasing floodplain water infiltration, referred to as the flood pulse (Junk *et al.*, 1989), is a process-based approach to increasing fine sediment delivery to floodplains. The complex nutrient cycling that occurs during overbank flooding and the near-channel water exchange that occurs through down-welling and up-welling at high flows are essential to maintaining river biodiversity (Stanford and Ward, 1988; Wyatt *et al.*, 2008).

The recent transition from form-based to process-based river restoration is supported by a growing body of literature emphasizing the importance of three types of river connectivity: upstream–downstream, river–riverbed, and river–floodplain (Findlay, 1995; Kondolf *et al.*, 2006; Wohl *et al.*, 2015; Covino, 2017). Reconnecting the river with the surrounding floodplain is a common goal in restoration. Overbank flooding is one mechanism by which this connectivity occurs, but subsurface mixing of stream water with groundwater, called hyporheic exchange, is another important connectivity process. As water moves between the stream sediments and the shallow groundwater, important biogeochemical reactions occur, including nutrient cycling (Boano *et al.*, 2014) and denitrification (Gomez-Valez *et al.*, 2015). Recent hydrologic research within the hyporheic zone has employed shallow geophysical techniques such as seismometers to measure discharge (Anthony *et al.*, 2018) or electrical resistivity to measure hyporheic exchange (Ward *et al.*, 2010a, 2010b). The use of shallow geophysics in restoration applications is still relatively uncommon, however, but electrical resistivity is widely used in other subsurface hydrology characterizations because large spatial coverage and high temporal resolution can be achieved through non-destructive means (Johnson *et al.*, 2012). Toran *et al.* (2012) used electrical resistivity during a surface tracer test to assess changes in the hyporheic zone induced by an in-stream restoration structure. In other scenarios, electrical resistivity analyses have been paired with surface salt tracer tests to characterize solute transport and/or hyporheic exchange (Ward *et al.*, 2010b, 2014; Cardenas and Markowski, 2011; Johnson *et al.*, 2012). Conservative tracer injections are more commonly used to characterize gross hydrologic exchanges between montane streams and adjacent groundwater (Covino *et al.*, 2011; Harman *et al.*, 2016).

We present a case study from a montane wetland on the Upper Colorado River in north-central Colorado where electrical resistivity was combined with a salt tracer test in a restoration environment. In May 2003, a debris flow initiated from Grand Ditch, a water diversion structure on the hillslope above Lulu City Wetland within the Never Summer Mountains in Northern Colorado (Figure 1). The event introduced 36 000 m^3 of sediment into the Upper Colorado River valley, including 1 m of sands and gravels deposited into Lulu City Wetland during snowmelt runoff (Rathburn *et al.*, 2013). By 2015, sediment deposition at the head of the wetland, which continued each year during snowmelt runoff, had increased sheet flow and decreased continuous perennial streamflow, thereby disconnecting the water table from the soil surface (RMNP, 2013). To fulfill requirements of a civil settlement reached with owners and operators of Grand Ditch, Rocky Mountain National Park staff developed a plan to restore the natural hydrologic processes, ecological function, and wilderness character to Lulu City Wetland (RMNP, 2013).

We used pre- and post-restoration measurements to assess surface water–groundwater exchange and in-channel storage potential in this river–wetland system. To the best of our knowledge, this is the first time the combination of a water balance, hydrologic tracer, and shallow geophysical surveys have been used to assess the effects of channel restoration on wetland water storage. To this end, we focused on two objectives: (1)

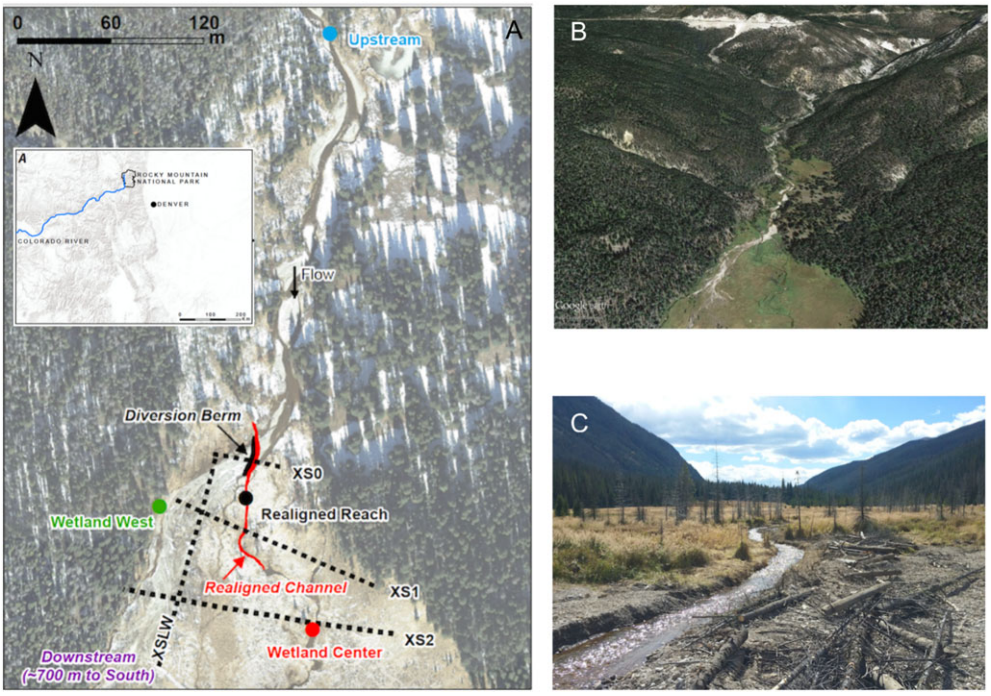

Figure 1. The Upper Colorado River and northern extent of Lulu City Wetland, Rocky Mountain National Park. Panel A: Annotated 2012 ortho-image of the study area. A-inset shows the location of Rocky Mountain National Park. Circles indicate monitoring site locations. Dotted lines indicate electrical resistivity transects. The Realigned Channel and associated diversion berm are also indicated. Not pictured is the Downstream monitoring site on the Colorado River, 700 m to the south. Panel B: oblique aerial image of Lulu City Wetland, showing debris flow sediments in gray, and the debris flow scar 2 km to the north. Panel C: view to the south (downstream) showing the constructed diversion berm and Realigned Channel; photo date 4 October 2015. [Colour figure can be viewed at wileyonlinelibrary.com]

quantifying changes in the surface water flux through an unconfined wetland following channel restoration; and (2) identifying changes in hyporheic exchange caused by channel restoration.

Study Area

The Upper Colorado River flows through Lulu City Wetland in Rocky Mountain National Park (Figure 1). Within the wetland, the Colorado River is a multi-thread, meandering channel with a mixed sand-and-gravel bed and width-to-depth ratio between 3.8 and 5.8. Lulu City Wetland is 800 m long and 200–300 m wide with an upstream drainage area of 29 km^2. Valley sediment deposits in the upper 4 m of the wetland are spatially heterogeneous, composed primarily of sand (coarse to fine), silty clays, and peat layers (Rubin *et al.*, 2012). Total sediment thickness has not been measured within Lulu City Wetland, but down-valley seismic surveys estimate depths to bedrock between 15 and 122 m below the present-day surface (Braddock and Cole, 1990). Lulu City Wetland receives an average of 66 cm of precipitation per year, the majority of which falls as snow between October and May (SNOTEL site 688, NRCS, 2016). Peak flows on the Upper Colorado River usually occur in early to mid-June, and Grand Ditch diverts up to 50% of snow runoff out of the Upper Colorado Basin (Clayton and Westbrook, 2008). The geology underlying portions of Grand Ditch upstream of Lulu City Wetland is primarily Tertiary rhyolite tuff (Braddock and Cole, 1990), which has been weathered *in situ* by hydrothermal alteration (Grimsley *et al.*, 2016). Beginning with the start of construction on Grand Ditch in 1890, augmented peak discharge and increased debris flows have altered the ecology and geomorphology of the Colorado River in Lulu City Wetland (Clayton and Westbrook, 2008; Rathburn *et al.*, 2013; Grimsley *et al.*, 2016). The human imprint on Lulu City Wetland extends long before the construction of Grand Ditch, as the Upper Colorado River valley supported various native peoples since the last glacial maximum and intermittent mining camps in the early 19th century (Andrews, 2011).

In September 2015, Rocky Mountain National Park staff diverted and realigned the Colorado River where it flows into Lulu City Wetland. This restoration consolidated two prominent flow paths (referred hereafter as West and Center channels) into one channel (Center) by a 27 m long earthen berm and a 190 m constructed channel (Realigned Channel) (Figure 1(a); Figure 2). The West Channel was 840 m long and straight (sinuosity = 1.2) and the Center Channel is 1100 m long and more sinuous (sinuosity = 1.5). The bed slope of the Realigned Channel originally had an average slope of 1.9%, which was steeper than the 1.0% slope of the West Channel it replaced. The Realigned Channel was dug by hand to an average width of 1.6 m and average depth of 0.4 m. The Realigned Channel was excavated into an area heavily vegetated by sedges (*Carex utriculata* and *Carex aquatilis*) and tall grass (*Calamagrostis canadensis*), and its depth was largely controlled by the depth required to remove the sedge root wads. The earthen diversion berm was built adjacent to the right bank of the Realigned Channel and diverted all but peak flows away from the pre-restoration West Channel (Figure 1(A); (C)). The berm had initial dimensions of 1 m high, 2 m wide, and 27 m long, and was built using ~30 m^3 of sand and gravel excavated from the constructed channel and topped with logs.

Methods

We used discharge measurements from the Colorado River and a NaCl tracer injection, paired with electrical resistivity, to characterize water storage and surface water–groundwater interactions within the river–wetland system. Discharge measurements were recorded at monitoring sites along the length of the Colorado River through Lulu City Wetland (Figure 2). Surface water salt concentrations were measured during and after the salt-tracer injection at selected monitoring sites used to measure discharge. Electrical-resistivity transects were chosen to maximize the spatial coverage in the northern portion of Lulu City Wetland exposed to debris-flow sediment deposition (Figure 1). The pre-restoration experiment was conducted 5–7

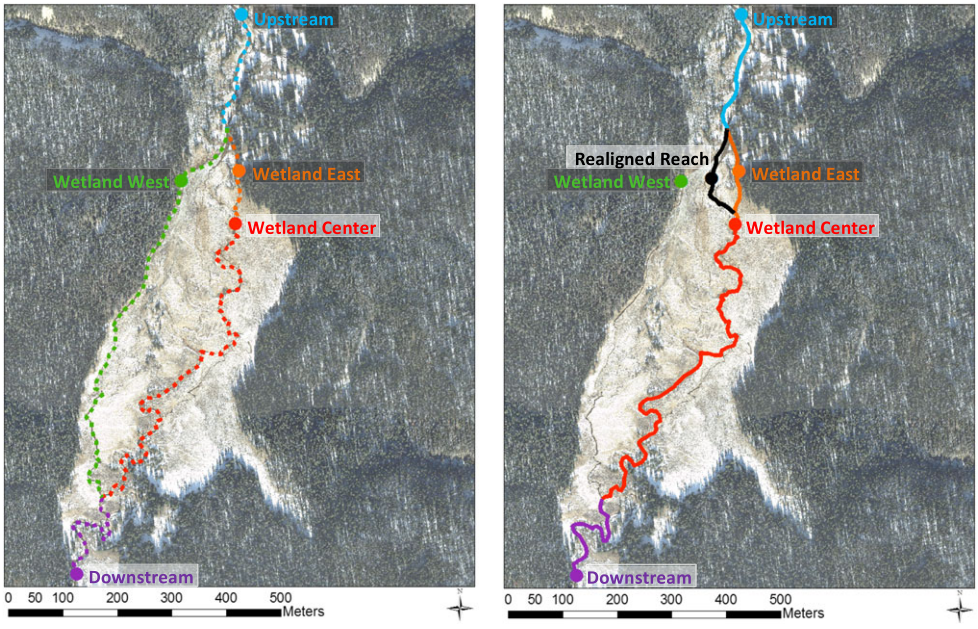

Figure 2. Major stream flow paths through Lulu City wetland. Pre-restoration flow paths are depicted in panel A and post-restoration flow paths are depicted in panel B. Circles indicate monitoring site locations. Colored lines indicate channels and are colored to match associated monitoring sites. In the text the green, red, and black lines are referred to as West Channel, Center Channel, and Realigned Channel, respectively. [Colour figure can be viewed at wileyonlinelibrary.com]

September 2015 and the post-restoration experiment was conducted 27–29 August 2016, using the 2015 protocol.

Field methods

Stage-discharge rating curves were used to estimate continuous discharge at the Upstream and Downstream monitoring sites. Discharge was also measured at intermediate monitoring sites during both experiments and used to calculate tracer mass recovery. Stream stage was recorded at 15 min intervals using Solinst Level Logger Edge Model 3001 pressure transducers (0.003 m accuracy). Discharge was calculated as the product of cross-sectional area and velocity. Velocity was measured with a Marsh McBirney FloMate Model 200 flow meter (2% accuracy) across the channel at an operator-defined interval that expressed relevant topographic changes and approximated equal percentages of flow in each measurement bin. Pre-restoration rating curves were constructed from four to six measurements, depending on monitoring site (Upstream: six measurements; Downstream: four measurements), and post-restoration rating curves were constructed from 10 measurements (both monitoring sites).

Channel cross-sections were relatively unstable, so we employed a hydraulic approach to compute stage-discharge relationships instead of a traditional statistical approach, which assumes that cross-section geometry does not change through time. Cross-section surveys, measured flow rates, and estimated roughness coefficients were used to compute corresponding hydraulic gradients assuming uniform flow concepts and the Manning equation. Uniform flow was a reasonable assumption at the monitoring sites on the Colorado River because they were located within a meandering, gravel/cobble-bed, pool–riffle system. The hydraulic approach was used to compute the range of flows that occurred within time periods constrained by the measured cross sections. Peak discharge could not be measured because the Colorado River was not wadable at high flows. Out of bank flows were therefore estimated (Supporting material, Table S1). The remoteness of the site made it difficult to transport or install infrastructure needed to measure high flows. During the pre-restoration measurement period, 17% of Upstream site discharge values and 53% of Downstream site discharge values were extrapolated beyond bankfull stage. During the post-restoration measurement period, 8% of Upstream site discharge values and 39% of Downstream site discharge values were extrapolated beyond bankfull stage. Discharge measurements were internally consistent between years and therefore introduced minimal error into subsequent analyses.

We injected the NaCl-stream water solution at the Upstream monitoring site at a constant rate of 10^{-4} m^3 s^{-1} for exactly 4 hours during base flow on 6 September 2015 (pre-restoration) and 28 August 2016 (post-restoration). Fluid electrical conductivity was monitored at the injection site, all intermediate monitoring sites within the wetland, and at the Downstream monitoring site (1590 m downstream from the injection site) (Figure 2). The concentration of the injected solution was 43 000 mg L^{-1} during the pre-restoration experiment and 46 000 mg L^{-1} during the post-restoration experiment, which was sufficient to raise stream concentrations enough above background to produce strong signals in fluid conductivity and bulk electrical resistivity measurements. Stream background concentration was 21 mg L^{-1} during the pre-restoration experiment and 23 mg L^{-1} during the post-restoration experiment. Discharge at the Upstream monitoring site was measured at 0.061 m^3 s^{-1} during the pre-restoration experiment and 0.066 m^3 s^{-1} during the post-restoration experiment.

Salt recovery was assessed at monitoring sites through mass balance, following the technique used to characterize solute retention in other river systems (Wondzell, 2006; Covino *et al.*, 2011). During the tracer test, Onset HOBO model U24 conductivity probes (3% or 20 µS cm^{-1} accuracy) were used to measure the specific conductivity of surface water (fluid electrical conductivity). Specific conductivity was an appropriate proxy measurement for NaCl concentration because strong linear relationships existed (r^2>0.999) across the conductivity probes used (NaCl=[0.47–0.51] SC + [0.08–0.94]). Probes were calibrated using a six-point standard curve that incorporated the range of field-measured values.

Electrical resistivity was used to observe areas within the hyporheic zone where exchange occurred between salt-traced stream water and natural groundwater. Because electrical resistivity is an intrinsic measure of a material's resistance to electric current flow, low electrical resistivity indicates highly conductive, saturated or moist soil, while high electrical resistivity indicates less conductive, drier substrate. By measuring changes in electrical resistivity relative to background through time, we were able to identify the active hyporheic zone, where surface water exchanged with groundwater. Electrical resistivity transects were measured using an IRIS Syscal Pro resistivity meter and stainless-steel electrodes placed along linear transects. Groupings of four electrodes, called quadripoles, were used as suggested by Ward (1990) to generate data along the transect according to a user-defined program based on a dipole–dipole measurement scheme and two-measurement stacking.

Each transect included 2595 quadripoles, but the number of surface electrodes varied between 48 and 72, depending on the electrode spacing (between 1 and 4 m) and desired resolution. In general, close electrode spacing allows for higher-resolution imaging of shallow subsurface resistivity than wide electrode spacing (Binley and Kemna, 2005). For example, a transect with 48 electrodes and 1 m spacing would include 2595 quadripoles over a transect length of 48 m. This array would provide greater resolution than a transect with 48 electrodes and 4 m spacing, which would include the same number of quadripoles (2595), but would cover a longer transect distance (192 m).

The dipole–dipole survey method was chosen for its ability to resolve vertical features and tracer plumes better than other electrical resistivity survey methods (Binley and Kemna, 2005), although it is subject to signal-noise issues because measurement electrodes are positioned outside of the pair of transmitting electrodes (Ward, 1990). Under the dipole–dipole scheme one electrode pair was used to drive current and nine others were used to measure the difference in potential, each of which was then used to calculate a resistance measurement used in inversion (Binley and Kemna, 2005).

During both tracer experiments, which were completed along transect XS1 (Figure 1), the electrode spacing was 4 m across the Realigned Channel and 1 m across each of the Center and West Channels. Twenty-eight electrical resistivity surveys were completed during the pre-restoration experiment and 31 were completed post-restoration. Each electrical resistivity survey required, on average, 37 min to complete under pre-restoration conditions and 24 min under post-restoration conditions. Background data were collected along transect XS1 before the salt tracer experiments and served as the baseline against which electrical resistivity changes were compared. During each experiment, electrical resistivity data were recorded continuously along transect XS1 for 20 h after the start of the tracer injection.

Three additional electrical resistivity transects within Lulu City Wetland were measured (XS0, XS2, XSLW) (Figure 1) in the same locations as ground-penetrating radar transects that

Rubin *et al.* (2012) used to map valley-bottom sediments. Electrode positions for all transects were surveyed using a Topcon GR-5 real time kinematic global navigation satellite system (0.01 m horizontal and 0.015 m vertical accuracy).

Data analysis

Discharge data from the wetland input (Upstream monitoring site) and output (Downstream monitoring site) were used to calculate hydrologic flux through the wetland. This technique was used by Wegener *et al.* (2017) to characterize water sources and sinks in a similar unconfined montane river valley. Daily discharge values were normalized by drainage area (Upstream drainage area = 25.5 km^2; Downstream drainage area = 29.1 km^2) and reported as runoff rate (mm day^{-1}). Daily flux values were calculated by subtracting the daily input discharge from the daily output discharge. Negative fluxes indicate surface water loss, primarily to groundwater or through evapotranspiration and in-channel storage, while positive fluxes indicate surface water gains from groundwater, tributaries, or less loss to storage.

Solute tracer breakthrough curves were created for all monitoring sites for the duration of each experiment and continuing for 20 h. Tracer mass recovery (T_{MR}) was calculated at each location by integrating the area under the tracer concentration breakthrough curve (concentration time series) using Equation (1):

$$T_{MR} = Q\int_0^t T_c(\tau)d\tau \quad (1)$$

where Q is measured discharge; T_c is the background corrected instantaneous tracer concentration (mg L^{-1}); and t is the time of the experiment from injection (τ=0) to return to background (τ=t). Tracer travel times were used to characterize the transport through the river–wetland system. We compared the commonly used metrics of arrival time (5% mass recovery), time to median (50% mass recovery), departure time (95% mass recovery), and time to peak tracer concentration (Runkel, 2015).

Gross discharge gains and losses were calculated during the experiments using upstream and downstream discharge and fractional tracer mass loss, after Covino *et al.* (2011). Net change in discharge (NetΔQ) was calculated:

$$Net\Delta Q = Q_{DS} - Q_{US} \quad (2)$$

where Q_{US} is upstream discharge and Q_{DS} is downstream discharge. Gross discharge loss (Q_{loss}) was calculated:

$$Q_{loss} = Q_{US} * \%T_{ML} \quad (3)$$

where $\%T_{ML}$ is *100%- $\%T_{MR}$*, as a fraction of the added mass and gross discharge gain (Q_{gain}) was calculated by mass balance:

$$Q_{gain} = Net\Delta Q + Q_{loss} \quad (4)$$

Equation (3) is an estimate of water volume loss associated with tracer mass loss, subject to uncertainty caused by the unknown order of gross gains and losses over the study reach. This equation quantifies the minimum water loss associated with a given tracer loss, because it assumes all loss occurs before all gain, and thus all the water is lost when the tracer is at its maximum concentration (before any dilution by gross gains). Any tracer loss occurring after dilution by gross gains would require a larger volume of water loss to result in the same mass of tracer loss. The difference between minimum and maximum estimates of gross loss can be quite large for reaches with large gross gains. Here, we use the minimum as the conservative estimate to avoid overestimating the influence of surface–subsurface exchanges.

Maps of subsurface bulk electrical conductivity (tomograms) were generated along each electrical resistivity transect through data inversion using the code R2 (Binley, 2016). The R2 code adjusted data weights, based on stacking errors, to produce electrical resistivity inversions such that the ratio of root mean square error (RMSE) to noise was optimized to the value nearest unity. The reciprocal of bulk electrical resistivity, bulk electrical conductivity, was used for interpretation.

Inverted electrical resistivity data along the east–west transect XS1 were used to compare relative changes in active hyporheic zone area through time and between experiments. The active hyporheic zone was defined as the area within the larger hyporheic zone subjected to increases in bulk electrical conductivity related to tracer water exchange with groundwater. Three segments along transect XS1 were used for this analysis, including 12–22 m (centered on the Center Channel), 70–95 m (centered on the Realigned Channel), and 121–131 m (centered along the West Channel).

Results

Wetland discharge

Pre- and post-restoration discharges were compared between the Upstream and Downstream monitoring sites to assess changes in wetland storage between experiments. Peak discharge in 2016 at both the Upstream and Downstream monitoring sites was higher than in 2015 (Figure 3). Rising and falling limbs at both sites were steeper and total discharge higher in 2016 than in 2015. The 2016 snow pack peaked at 28 cm of snow water equivalent and melted faster than the 2015 snow pack, which peaked at 23 cm of snow water equivalent (NRCS, 2016). Even though peak discharges were smaller in 2015, they lasted longer into the summer. Rainfall was largely insignificant in both years, although early July rains resulted in a small secondary sub-peak in 2015. Despite the differences in snowmelt amount and timing, the wetland surface water response was assumed to be similar between years, due to consistent Grand Ditch-related diversions that minimized the effects of inter-annual variations in snowmelt runoff.

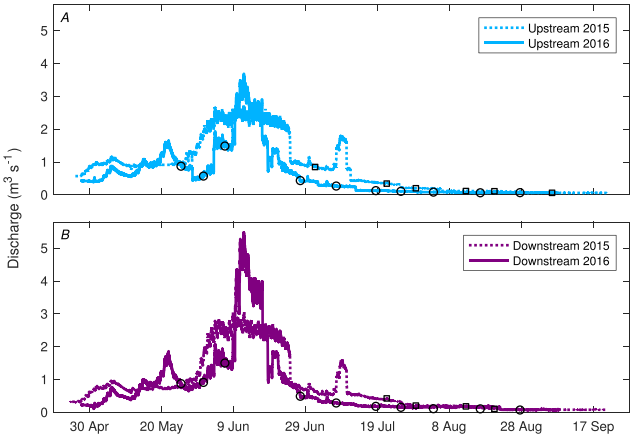

Figure 3. Flow hydrographs. Panel A: Upstream monitoring site. Panel B: Downstream monitoring site. Symbols indicate field measured discharge points (square = 2015, circle = 2016). [Colour figure can be viewed at wileyonlinelibrary.com]

Pre- and post-restoration discharge conditions at the Upstream monitoring site were similar during both experiments (0.061 m^3 s^{-1} and 0.066 m^3 s^{-1}, respectively), but pre-restoration discharge at the Downstream monitoring site was higher than post-restoration discharge (0.086 m^3 s^{-1} and 0.070 m^3 s^{-1}, respectively; Table I). When considered over the entire summer measurement period, the pre-restoration water flux balance in Lulu City Wetland was negative (inflow>outflow) in the early spring, positive (outflow>inflow) during snowmelt, and close to zero during baseflow (Figure 4(A)). Post-restoration, the positive flux balance during peak snowmelt was much higher than pre-restoration. Following snowmelt, the post-restoration wetland flux balance remained close to zero, while the pre-restoration balance became negative before returning to zero during base flow. The cumulative water flux balance through Lulu City Wetland showed large differences in summer water storage between experiments (Figure 4(B)). A net positive water yield indicates water export through the wetland and a net negative water yield indicates water storage in the wetland. The pre-restoration cumulative total water yield was –58 mm and the post-restoration cumulative water yield was 173 mm, resulting in a between-year change in water yield of 231 mm (Figure 4(B)). The additional 231 mm suggests a decrease in wetland water storage following restoration. We do not consider evapotranspiration differences to be a factor in differences in wetland discharge between the two years because of similar pre- and post-restoration controls on evapotranspiration. Gross gains did not change between experiments but gross losses increased from 0.005 m^3 s^{-1} to 0.027 m^3 s^{-1}, resulting in lower net gains post-restoration compared with pre-restoration (Table I). Gross gains and losses during the experiments differ from the wetland water flux because they describe how solute traced water moved through storage during the experiment measurement period.

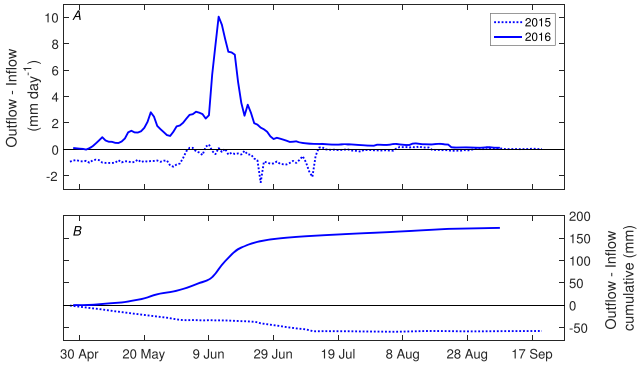

Figure 4. Discharge through Lulu City Wetland. Panel A: The daily pre- (2015) and post- (2016) restoration discharge was calculated by subtracting the normalized daily discharge at the Upstream site from the normalized daily discharge at the Downstream site. Panel B: Cumulative pre- (2015) and post- (2016) restoration discharge through the wetland. [Colour figure can be viewed at wileyonlinelibrary.com]

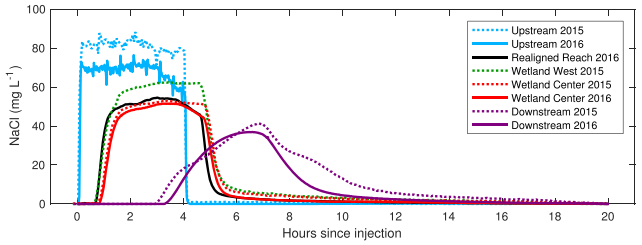

Figure 5. Salt tracer breakthrough curves at the stream monitoring sites within Lulu City Wetland. Background concentrations were adjusted to zero mg L^{-1} to allow for between-site comparisons. Legend entries are listed by river distance from the Upstream site: Wetland East = 310 m, Realigned Reach = 325 m, Wetland West = 365 m, Downstream = 1590 m. The prerestoration experiment occurred in 2015; the post-restoration experiment occurred in 2016. The Realigned Reach did not exist in 2015 and the Wetland West monitoring site was completely dry in 2016. [Colour figure can be viewed at wileyonlinelibrary.com]

Tracer breakthrough curves

Tracer breakthrough curves for the duration of the salt tracer test are presented in Figure 5. Higher post-restoration base flow discharge at the Upstream monitoring site resulted in a slightly lower plateau concentration compared with the pre-restoration plateau concentration. The plateau variance shown in the Upstream breakthrough curve during both experiments was a result of incomplete mixing. Day (1977) found that a downstream mixing length of 25 times the channel width was adequate for complete vertical and lateral mixing for salt during dilution gaging experiments in mountain streams. The mixing length in the Upstream Channel was limited to 12.5 times river width to ensure that surface fluid conductivity was measured upstream of the transition to distributary channels and multi-threaded flow that occurred 35 m downstream of the Upstream monitoring site.

The effects of light rainfall that occurred during the post-restoration experiment can be seen in the breakthrough curve plateau (Figure 5). Rain began 2.5 h into the tracer injection and lasted through the end of the injection at 4 h; however, 15 min stage measurements indicate that river flow did not increase during the storm. Because all analyses of tracer recoveries were based on the mass recovery at the Upstream monitoring site during the experiment, it was not imperative that concentrations between experiments were exactly the same. More importantly, the timing and slope of the rising and falling limbs within the Upstream breakthrough curves were identical in each experiment, as were the magnitude and variance within each plateau (Figure 5).

The Downstream breakthrough curves did not show the plateau shape typical of constant-rate injections in either experiment (Figure 5). Slope changes on both the rising and falling limbs of the pre-restoration Downstream breakthrough curve were notable when compared with the post-restoration Downstream breakthrough curve, where they were entirely absent (Figure 5). The rising limb slope change indicates earlier pre-restoration tracer arrival and the falling limb slope change

Table I. Total discharge, gross discharge gain, gross discharge loss, and tracer velocity through Lulu City Wetland during pre- (2015) and post- (2016) restoration salt-tracer injection experiments. A velocity range is listed in 2015 because two active channels (West and Center) of different flow lengths transported water through the wetland at different velocities

Date	Upstream Q (m^3 s^{-1})	Downstream Q (m^3 s^{-1})	Net change in Q (m^3 s^{-1})	Q_{gain} (m^3 s^{-1})	Q_{loss} (m^3 s^{-1})	Median tracer velocity ($m\,h^{-1}$)
6 Sep 2015	0.061	0.086	0.025	0.030	–0.005	2.5–3.0
28 Aug 2016	0.066	0.070	0.004	0.030	–0.027	3.3

indicates greater pre-restoration hydrologic retention upgradient from the wetland outlet. The remaining monitoring sites exhibited plateau breakthrough curve patterns that were similar across sites and between years. Lower plateau concentrations at these intermediate sites reflected varying degrees of dilution from groundwater inputs.

Tracer mass recovery

Mass recovery decreased between pre- and post-restoration experiments through the West Channel and mass recovery increased through the Center Channel (Figure 6). The combined mass recovery at the Wetland West and Wetland Center monitoring sites prior to restoration totaled 70% of the mass injected at the Upstream monitoring site (Figure 6). Following restoration, 108% of injected mass was recovered at the Wetland Center monitoring site (Figure 6), suggesting a strong influence of channelization and consolidation of flow through the Realigned Channel resulting from the diversion berm. Compounded instrument error, paired with measurement uncertainty and background interpolation, might explain the >100% mass recovery value. Diel fluctuations in fluid conductivity, which were not measured prior to salt tracer injection, may have also contributed to a high bias in mass recovery value. For interpretation, mass recovery at the Wetland Center monitoring site was treated as 100%. Mass recovery at the Downstream monitoring site decreased following restoration; 91% of injected mass was recovered prior to restoration and only 59% was recovered post-restoration (Figure 6).

Pre- and post-restoration tracer travel times, taken from the cumulative mass time series (Figure 7), are listed for the Downstream monitoring site in Table II. The post-restoration tracer arrival time was 16 min slower and the post-restoration departure time was 145 min faster than equivalent pre-restoration travel times. The post-restoration median travel time was 44 min faster than the pre-restoration median travel time. The post-restoration peak concentration occurred after the post-restoration median accumulation and prior to the pre-restoration median accumulation.

Electrical resistivity

Fence diagrams were used to display the electrical resistivity transects in 3-dimensional space within Lulu City Wetland (Figure 8). This particular representation highlights broad changes in bulk electrical conductivity related in part to sediment characteristics throughout the study area, but is not sensitive enough to accurately identify small-scale changes in substrate that may influence

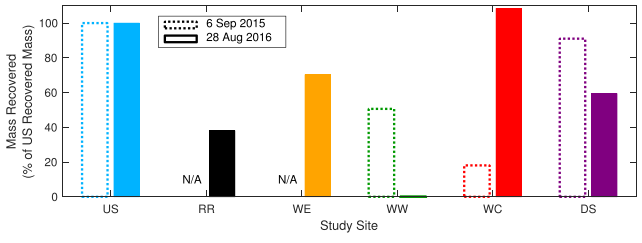

Figure 6. Salt tracer test mass recovery by monitoring site within Lulu City Wetland, Rocky Mountain National Park. Open bars are pre- (2015) restoration and closed bars are post- (2016) restoration experimental data. US = Upstream; RR = Realigned Reach; WE= Wetland East; WW = Wetland West; WC = Wetland Center; DS = Downstream Site. 'N/A' indicates sites for which mass recovery was not calculated in 2015. The Realigned Reach site did not yet exist. The Wetland East site was not monitored due to equipment limitations. [Colour figure can be viewed at wileyonlinelibrary.com]

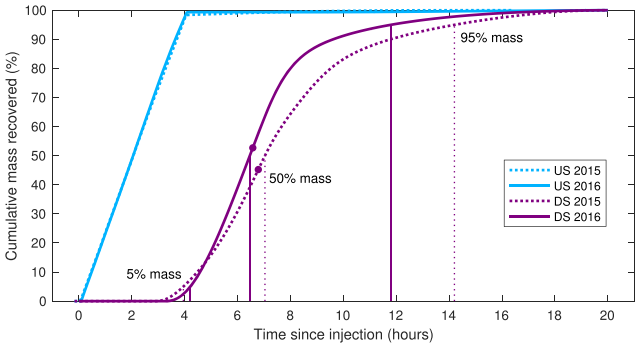

Figure 7. Cumulative mass recovery at the Upstream (US) and Downstream (DS) monitoring sites within Lulu City Wetland, Rocky Mountain National Park. Downstream site salt recovery is expressed relative to the mass recovered at the Upstream site in each experiment. Vertical lines indicate tracer arrival (5%), median (50%) and departure (95%) times. Filled circles indicate peak concentration. Dashed lines indicate pre-(2015) restoration and solid lines indicate post- (2016) restoration experimental data. [Colour figure can be viewed at wileyonlinelibrary.com]

Table II. Characteristic travel times for Downstream monitoring site (wetland outlet) during the pre- (2015) and post- (2016) restoration tracer tests. Percentages reflect the portion of total mass recovered at the Downstream monitoring site during the experiment

Date	Time to 5% (min)	Time to 50% (min)	Time to 95% (min)	Time to peak (min)
6 Sep 2015	237	422	853	407
28 Aug 2016	253	378	708	395

hyporheic exchange. Bulk electrical conductivity was generally high in areas under the flowing Colorado River in the Center Channel and portions of the West Channel. Bulk electrical conductivity remained relatively low under the Realigned Channel following restoration, even though surface water flowed through the open channel (Figure 8(B)).

Artifacts of post-processing often obscure accurate bulk electrical conductivity interpretations near the edges of transects. The potential fields measured during electrical resistivity procedures extend in three dimensions, but tomograms compress that information into a 2-dimensional representation (Nimmer *et al.*, 2008). These 'out-of-plane' effects may explain why bulk electrical conductivity was lower along the valley length transect (XSLW) than the east–west transect (XS0) at the intersection of those two transects in the northern part of Lulu City Wetland (Figure 8). Along the valley-length transect (XSLW), bulk electrical conductivity was highest at intersections with the West Channel and XSO, both near the northern extent of XSLW. Comparatively little change in bulk electrical conductivity occurred between pre- and post-restoration experiments in the Realigned Channel, which suggests limited spatial influence of the new channel on the surrounding shallow groundwater.

Changes in active hyporheic zones within the Center, Realigned, and West channels during the experiments are shown, along with tracer breakthrough curves from associated monitoring sites (Wetland Center, Realigned Reach, and Wetland West), in Figure 9. The pre-restoration condition was included for the Realigned Channel and Realigned Reach monitoring site to show that bulk electrical conductivity was equivalent to background prior to the construction of the Realigned Channel. The post-restoration condition for the West Channel and Wetland West monitoring site was included to show a complete return to background following West Channel de-watering due to construction of the earthen diversion berm.

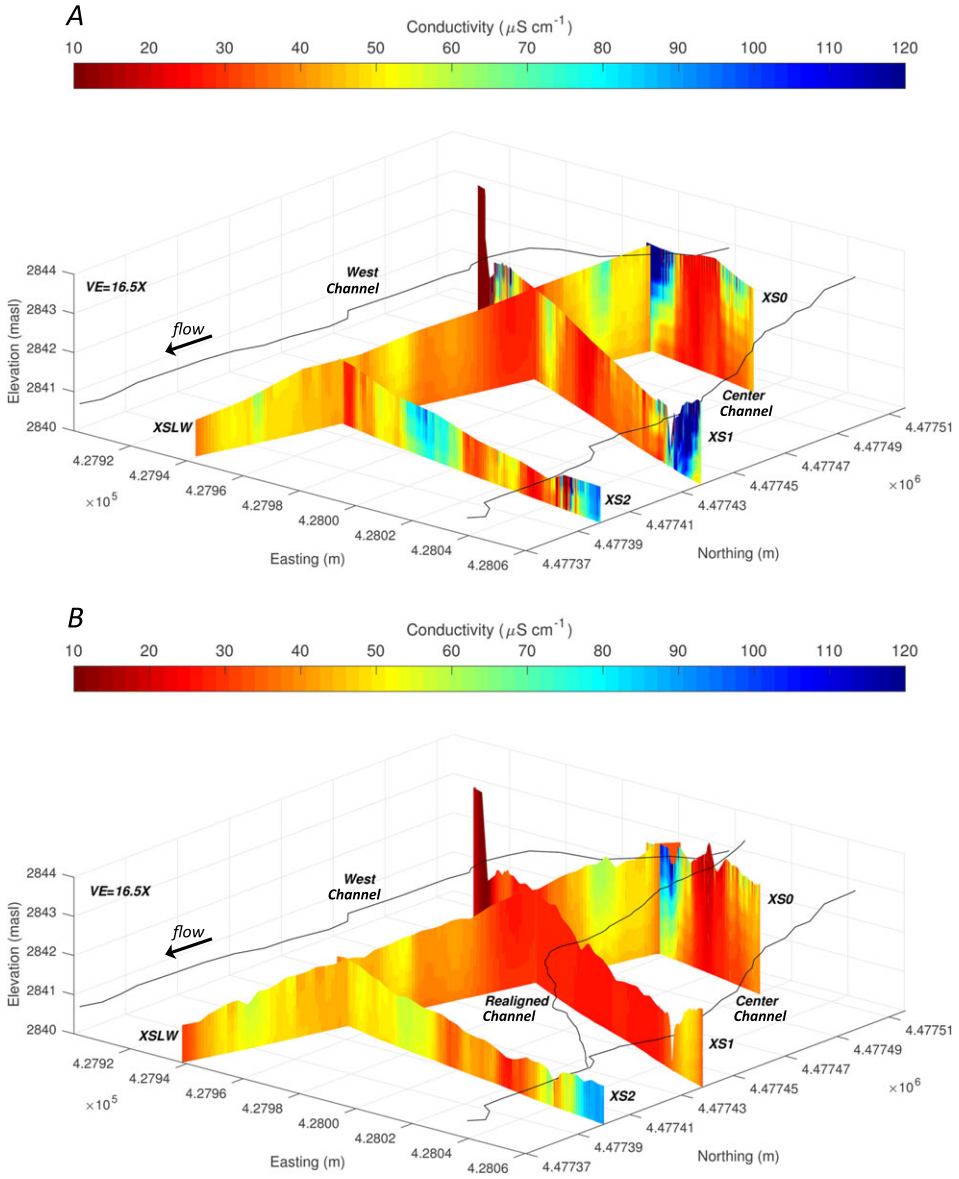

Figure 8. Electrical resistivity transect tomograms in 3-dimensional space within the pre-restoration (Panel A) and post-restoration (Panel B) Lulu City Wetland. Stream channels are added for reference; stream flow is from north to south. The view orientation is from an azimuth of 40° and elevation angle of 50°. [Colour figure can be viewed at wileyonlinelibrary.com]

Pre-restoration bulk electrical conductivity increased under the Center Channel during the first 3 h of the tracer test (Figure 9(B)). The active post-restoration portion of the hyporheic zone was smaller and more transient, and was not active until later during the falling limb of the tracer breakthrough curve (Figure 9(C)). Under the West Channel, pre-restoration bulk electrical conductivity increased for longer periods of time (Figure 9(J)–(L)). There was no post-restoration response under the West Channel during the same time period. No changes in bulk electrical conductivity were observed under the Realigned Channel between pre- and post-restoration conditions (Figure 9(E)–(H)). Changes in bulk electrical conductivity occurred within the first 6 hours of salt injection, after which bulk electrical conductivity returned to background concentrations.

Discussion

Substrate and geomorphic factors, including grain size and distribution (Valett *et al.*, 1996), sinuosity (Boano *et al.*, 2006), bed topography (Harvey and Bencala, 1993), and hydraulic head (Menichino and Hester, 2014) have been shown to affect hyporheic exchange in other river and wetland systems. Fluid and bulk electrical conductivity results from the Lulu City Wetland suggest an overall decrease in hyporheic exchange and wetland storage capacity between pre- and post-restoration conditions along the Upper Colorado River. We interpret the changes between the pre- and post-restoration conditions to result from variations in substrate characteristics and channel morphology. Competing feedbacks between changes in substrate characteristics and channel morphology make identifying direct cause and effect difficult in a complex system like Lulu City Wetland, however.

Substrate characteristics

Differences in the spatial distribution of substrate grain sizes may explain why the post-restoration tracer departure time at the Downstream site occurred more than 2 hours before the pre-restoration tracer departure time (Figure 7). Before restoration the Downstream monitoring site received surface water inputs primarily from two channels, West and Center (Figure 2). The pre-restoration West Channel flowed over

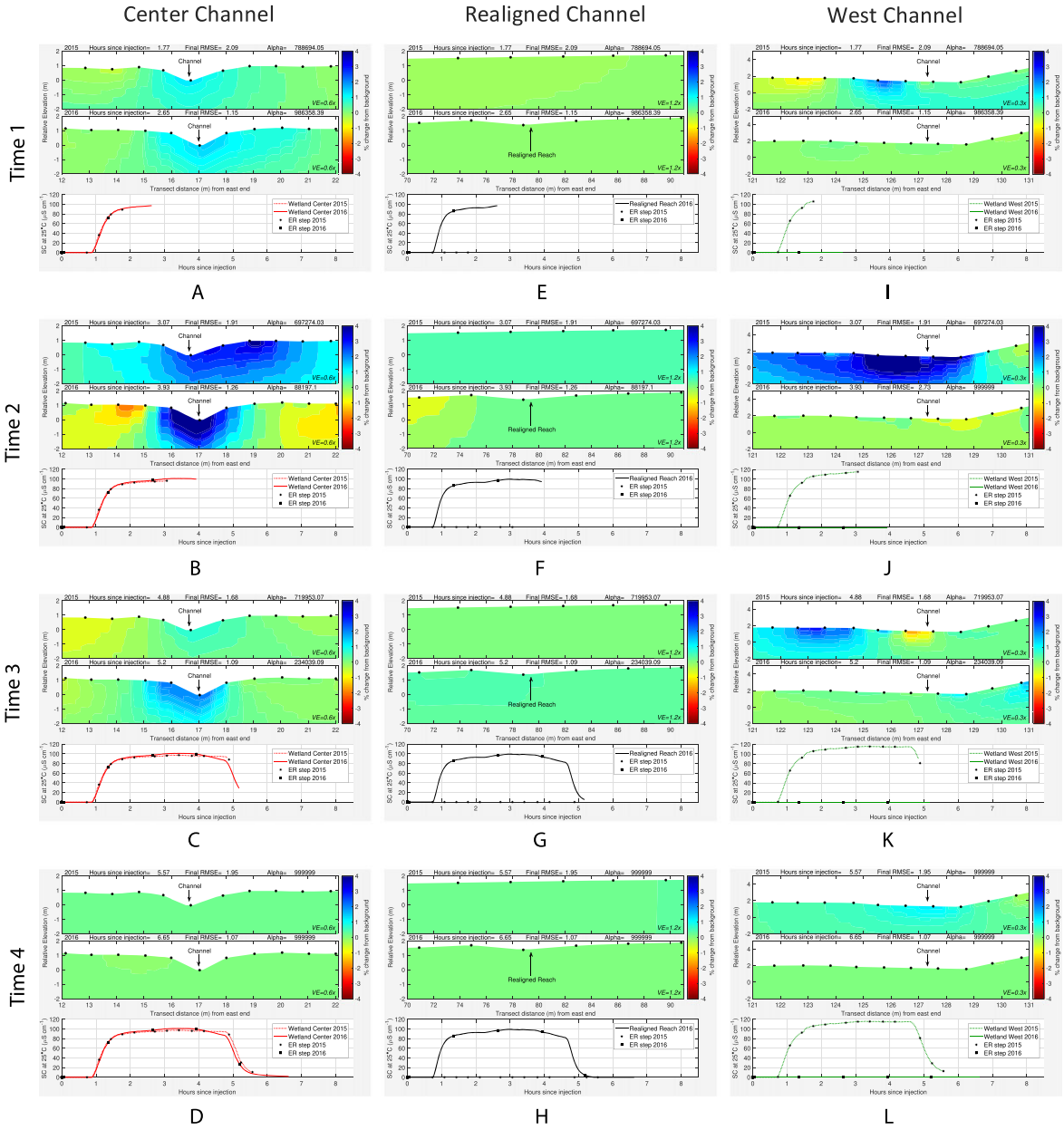

Figure 9. Comparative tomograms and tracer breakthrough curves from selected time steps during the electrical resistivity tracer tests. Panels A to D depict the Center Channel; Panels E to H depict the Realigned Reach; panels I through L depict the West Channel. Tomograms depict the change in bulk electrical conductivity from a background condition, measured along the electrical resistivity tracer transect (XS1). In each panel, the top frame is pre-restoration, the middle frame is post-restoration, and the bottom frame shows the solute breakthrough curve measured at the associated monitoring site, with electrical resistivity (ER) survey time steps marked. The background condition was established for each experiment prior to tracer injection. During the restoration, the Realigned Channel was constructed and the West Channel was de-watered. Tomogram time step, final RMSE (indication of model fit) and alpha (smoothing factor) are included. [Colour figure can be viewed at wileyonlinelibrary.com]

debris-flow sediments consisting of poorly sorted coarse sand, gravel, and cobbles while the Center Channel flowed over peat and fine-grained overbank deposits (Rubin *et al.*, 2012). Consequently, the hydraulic conductivity of the 2003 and earlier debris flow deposits under the West Channel would have been on the order of 30 times greater than that of the peat and over-bank deposits under the Center Channel, based on hydraulic conductivity estimates from the literature (EPA, 1986). Such permeable debris flow sediments may have controlled the hyporheic exchange observed under the West Channel during the pre-restoration experiment, where water flowed through diffuse subsurface flow paths. Because a large portion of flow entered and traveled through the hyporheic zone under the West Channel, salt-traced water was delayed in reaching the Downstream monitoring site. The delay as water was slowly released from storage can be seen in the falling limb slope change on the pre-restoration Downstream breakthrough curve (Figure 5).

Hyporheic exchange was observed as elevated bulk electrical conductivity, relative to background, in the Center Channel during both experiments. Pre-restoration increases in bulk electrical conductivity along the Center Channel (Figure 9(B) top) were measured on the rising limb of the breakthrough curve, when transport probably occurred through advective flow paths. Post-restoration increases in bulk electrical conductivity (Figure 9(B) and (C), middle) were less extensive and concentrated later on the plateau and on the falling limb of the tracer breakthrough curve, suggesting a transition to longer-term flow paths. While longer-term flow paths would still be beneficial to processes associated with hyporheic exchange, results from the salt-tracer suggest a decrease in the spatial and temporal extent of the hyporheic exchange

observed following restoration. At the Wetland Center monitoring site, the tracer plateau was shorter and the falling limb steeper during the post-restoration experiment (Figure 5), indicating rapid transport of the salt pulse through the Center Channel following restoration, and less water moving through slower, storage-related flow paths. Surface water diversions resulting from the constructed earthen berm increased both water volume and velocity through the Center Channel, which explains the shorter salt concentration plateau. Flow through the newly formed Realigned Channel eroded its bed and transported sediment downstream. We noted extensive winnowing of fine sediment during and after construction of the Realigned Channel and fine sediment deposition downstream near the Wetland Center monitoring site. In other systems with a large supply of fine sediment, infilling of coarse bed material has been shown to limit hyporheic exchange through the bed by creating smooth, impermeable surfaces (Boulton *et al.*, 1998).

Channel morphology

Our data indicate that construction of the earthen diversion berm at the head of the West Channel, and the associated construction of the Realigned Channel, altered channel morphology in ways that contributed to decreasing hyporheic exchange. The West Channel was straight, wide, and shallow (Figure 2; Figure 10), a combination of morphologically simple factors that are not usually the main drivers of hyporheic exchange. Meander bends generally increase hyporheic exchange (Boano *et al.*, 2006), but the apparent lack of hyporheic exchange observed at the more sinuous Center Channel and the extensive hyporheic exchange observed at the less sinuous West Channel suggest that substrate hydraulic conductivity had a greater effect than channel form on driving hyporheic exchange in Lulu City Wetland. This finding is further supported by the bulk electrical conductivity results within the area of the Realigned Reach monitoring site that show a lack of hyporheic exchange in post-restoration tomograms (Figure 9(E)–(H)). The Realigned Channel was also straight, shallow, and wide (190 m long, 1.4 m wide, 0.4 m deep) with similar substrate characteristics as the Center Channel.

A comparison of mass recovery at the Downstream monitoring site highlights the effect of channel morphology on hyporheic exchange at the wetland scale. High pre-restoration mass recovery (91%) and low gross discharge loss ($-0.005\ m^3\ s^{-1}$) at the Downstream monitoring site indicate that hyporheic exchange occurred on short time scales (Figure 6; Table I). Lower post-restoration mass recovery (59%) and increased gross discharge loss ($-0.027\ m^3\ s^{-1}$) indicate longer-term storage not related to hyporheic exchange within Lulu City Wetland. In a similar restored, low-gradient, headwater stream, Jefferson *et al.* (2013) found that hyporheic exchange was <1% of total transient storage whereas in a similar unrestored steam, hyporheic exchange accounted for up to 75% of total transient storage. Due to greater surface complexity within the Center Channel in (e.g. high sinuosity, side-channels), it is probable that some solute was stored within in-channel low-velocity areas, such as eddies and pools, for the duration of the measurement period. The remaining solute may have entered long, subsurface flow paths, where it did not rejoin surface flow in measureable concentrations during our monitoring period. Ward *et al.* (2010a) confirmed the presence of solute in slow, subsurface flow paths in similar systems long after stream solute concentrations had returned to background.

Surface complexity changes within the Center Channel may have altered how solutes were transported through Lulu City Wetland, but surface complexity did not have a similar effect on decreasing discharge through the wetland. The post-restoration water flux balance through the wetland was $10\ mm\ day^{-1}$ during peak flow compared with near zero during pre-restoration peak flow (Figure 4). This indicates that Lulu City Wetland exported more water during peak flow after the restoration, when surface water was consolidated in the single

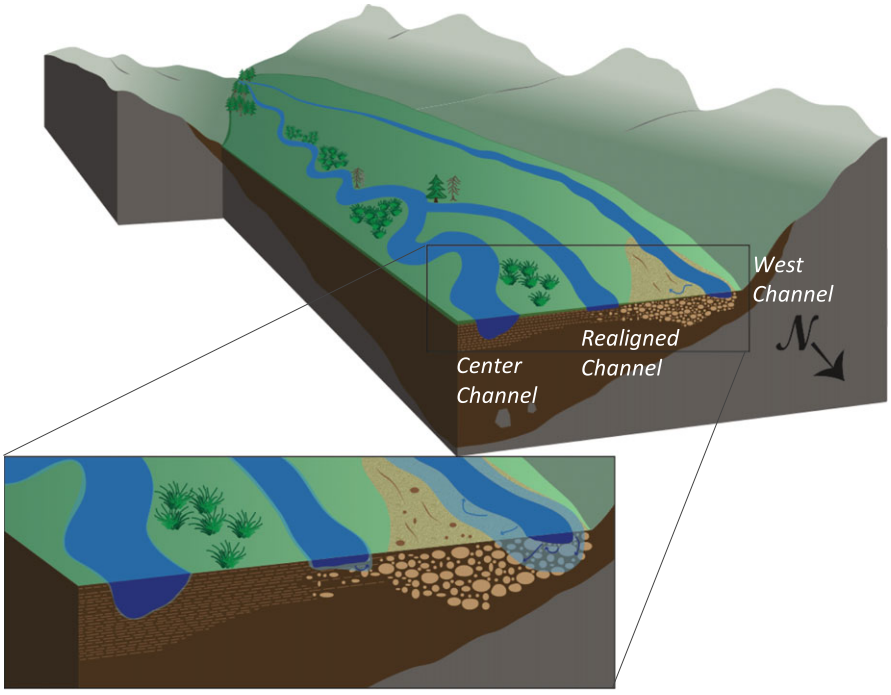

Figure 10. Conceptual representation of Lulu City Wetland, Rocky Mountain National Park, looking downstream. The Realigned and Center Channels are shown, as well as the West Channel that was blocked in 2015 by the construction of the diversion berm. Differences in substrate under each channel control the spatial extent and hydrologic characteristics of the active hyporheic zone, with flow paths indicated. [Colour figure can be viewed at wileyonlinelibrary.com]

Center Channel. Before the restoration, when the pre-restoration West Channel was active, water was distributed across the valley through overbank flooding, which increased infiltration and attenuated peak flows. Decreased water retention in Lulu City Wetland following restoration may have implications for infiltration and water storage in the river–wetland system. If the patterns of water export we observed 1-year post-restoration persist, water storage in the wetland may continue to decrease over the long term. A continuation of this trend could lower the water table and facilitate a shift in flora from wetland to upland species as has been seen in other wetland systems (Rood *et al*., 2003).

Management Implications

The loss of hyporheic exchange pathways, however small, is often detrimental to the biogeochemical processing, biodiversity, and river–floodplain connectivity in systems similar to Lulu City Wetland. Small-scale exchange pathways, which link gravel-bed rivers to their associated floodplains and adjacent riverbeds, are important for biodiversity and connectivity across the larger wetland system (Hauer *et al*., 2016). Zones of concentrated nutrients along the small hyporheic exchange flow paths affect flora and fauna on increasingly larger scales, ultimately influencing the biodiversity of the regional river–floodplain ecosystem (Wyatt *et al*., 2008).

Channel restoration often focuses on re-creating desired forms, like a straight, shallow channel, consistent meander bend, and constant channel slope, or on forcing a channel into a desired location like a historic flow path. These form-based goals have the potential to miss the process-based underpinnings that sustain fluvial systems. Restoration planners ought to consider that many restored systems are unable to provide the same level of ecosystem services or return to the equivalent level of biodiversity that undisturbed and natural wetlands offer (Zedler, 2004).

The restoration reviewed here is the first step in a larger project planned for Lulu City Wetland. This case study from the Upper Colorado River suggests that there may be unintended effects of form-based restoration on processes needed to support essential ecosystem services. Furthermore, this research helps provide a framework for estimating restoration targets in complex river–wetland systems. One year of restoration effectiveness monitoring from Lulu City Wetland highlights an important consideration for future wetland restoration projects: that form-based restoration may fail to address the processes needed to increase, or even maintain, surface water–groundwater interactions and associated ecosystem functions. In situations where restoration is needed, working with process and recovery are key premises of proactive river management (Brierley and Fryirs, 2009; Beechie *et al*., 2010). Furthermore, there is growing interest and effort in planning restoration approaches to enhance resilience (Tockner *et al*., 2000; Lake *et al*., 2007) and sediment recovery (Fryirs and Brierley, 2016; Rathburn *et al*., 2018) and in letting the river do the work.

In Lulu City Wetland, an alternative restoration approach could focus on limiting unnatural and excessive sediment inputs from Grand Ditch while also increasing water pulses to replicate natural peak flows. By simultaneously decreasing sediment supply and increasing sediment transport capacity, natural processes would, over time, restore sediment conditions within Lulu City Wetland to those that existed under the historic pattern of surface water–groundwater interactions. Such an approach would improve upon the reach-focused perspective by considering the longitudinal connectivity of river reaches as well as lateral connections with surrounding hillslopes.

Conclusion

In response to a breach in Grand Ditch, Rocky Mountain National Park constructed an earthen diversion berm and excavated a channel to realign a portion of the Upper Colorado River through a historic channel as it flows into Lulu City Wetland. The effects on hyporheic exchange were assessed in the first year following restoration. The channel realignment diverted flow from the pre-restoration West Channel and consolidated all river flow into the Center Channel. Hydrologic analyses indicate that this change increased water export through Lulu City Wetland by 231 mm, suggesting a decrease in wetland water storage capacity and lost potential for hyporheic exchange. Subsurface complexity appears to control hyporheic exchange more than surface complexity, as associated decreases in hyporheic exchange along the pre-restoration West Channel were not mitigated by equivalent increases in hyporheic exchange in either the Realigned Channel or Center Channel. By interpreting our results in the context of a larger river–wetland ecosystem, we discovered unintended consequences of prioritizing the restoration of river form over function and encourage restoration practitioners to consider the effects of form-based projects on water storage capacity in similar systems.

Acknowledgements—We thank Rocky Mountain National Park employees Paul McLaughlin and Scott Esser for facilitating this research. We are indebted to Jackie Randell without whom we could not have completed electrical resistivity measurements. We thank David Dust for field assistance and helpful discussions, as well as two anonymous reviewers whose comments greatly improved this manuscript. Additional thanks to summer field assistants Ford Fowler and Tyler Rich, and at least 30 people and three llamas who made this work possible. Funding was provided by Rocky Mountain National Park, CSU Warner College of Natural Resources and USGS through the CSU Water Center.

References

Andrews TG. 2011. An Environmental History of the Kawuneeche Valley and the Headwaters of the Colorado River, Rocky Mountain National Park [online] Available from: http://publiclands.colostate.edu/wp-content/uploads/2014/10/andrews-k-valley-eh-final-report-oct-6-2011.compressed.pdf (Accessed 19 May 2016)

Anthony RE, Aster RC, Ryan SE, Rathburn SL, Baker MG. 2018. Measuring mountain river discharge using seismographys emplaced within the hyporheic zone. *Journal of Geophysical Research: Earth Surface* **123**(2): 210–228. https://doi.org/10.1002/2017JF004295.

Beechie TJ, Sear DA, Olden JD, Pess GR, Buffington JM, Moir H, Roni P, Pollock MM. 2010. Process-based principles for restoring river ecosystems. *BioScience* **60**: 209–222. https://doi.org/10.1525/bio.2010.60.3.7.

Bernhardt ES, Palmer MA. 2011. River restoration: the fuzzy logic of repairing reaches to reverse catchment scale degradation. *Ecological Applications* **21**: 1926–1931. https://doi.org/10.1890/10-1574.1.

Binley A. 2016. R2, executable code [online] Available from: http://www.es.lancs.ac.uk/people/amb/Freeware/R2/R2_readme.pdf (Accessed 20 October 2016)

Binley A, Kemna A. 2005. DC resistivity and induced polarization methods. In *Hydrogeophysics*. Springer; 129–156. [online] Available from: http://link.springer.com/chapter/10.1007/1-4020-3102-5_5 Accessed 20 October 2016.

Boano F, Camporeale C, Revelli R, Ridolfi L. 2006. Sinuosity-driven hyporheic exchange in meandering rivers. *Geophysical Research Letters* **33**: L18406. https://doi.org/10.1029/2006GL027630.

Boano F, Harvey J, Marion A. 2014. Hyporheic flow and transport processes: mechanisms, models, and biogeochemical implications. *Reviews of Geophysics* **52**: 603–679. https://doi.org/10.1002/2012RG000417.

Boulton AJ, Findlay S, Marmonier P, Stanley EH, Valett HM. 1998. The functional significance of the hyporheic zone in streams and rivers.

Annual Review of Ecology and Systematics **29**: 59–81. https://doi.org/10.1146/annurev.ecolsys.29.1.59.

Braddock WA, Cole JC. 1990. *Geologic Map of Rocky Mountain National Park and Vicinity, Colorado* USGS, Denver, CO.

Brierley G, Fryirs K. 2009. Don't fight the site: three geomorphic considerations in catchment-scale river rehabilitation planning. *Environmental Management* **43**: 1201–1218. https://doi.org/10.1007/s00267-008-9266-4.

Cardenas MB, Markowski MS. 2011. Geoelectrical imaging of hyporheic exchange and mixing of river water and groundwater in a large regulated river. *Environmental Science and Technology* **45**: 1407–1411. https://doi.org/10.1021/es103438a.

Clayton JA, Westbrook CJ. 2008. The effect of the Grand Ditch on the abundance of benthic invertebrates in the Colorado River, Rocky Mountain National Park. *River Research and Applications* **24**: 975–987. https://doi.org/10.1002/rra.1117.

Cooper DJ, Chimner RA, Merritt DM. 2012. *Western Mountain Wetlands*. University of California Press: Berkeley, CA, USA.

Covino T. 2017. Hydrologic connectivity as a framework for understanding biogeochemical flux through watersheds and along fluvial networks. *Geomorphology* **277**: 133–144. https://doi.org/10.1016/j.geomorph.2016.09.030.

Covino T, McGlynn B, Mallard J. 2011. Stream-groundwater exchange and hydrologic turnover at the network scale. *Water Resources Research* **47** W12521. DOI: https://doi.org/10.1029/2011WR010942.

Dahl. 2000. Status and trends of wetlands in the conterminous United States 1986 to 1997. US Fish and Wildlife Service [online] Available from: http://repositories.tdl.org/tamug-ir/handle/1969.3/26244 (Accessed 6 January 2016)

Day TJ. 1977. Field procedures and evaluation of a slug gilution gauging method in mountain streams. *Journal of Hydrology* **16**: 113–133.

EPA. 1986. *Method 9100: Saturated hydrualic conductivity, saturated leachate conductivity, and intrinsic permeability*. US Environmental Protection Agency: Washington, DC.

Erwin KL. 2009. Wetlands and global climate change: the role of wetland restoration in a changing world. *Wetlands Ecology and Management* **17**: 71–84. https://doi.org/10.1007/s11273-008-9119-1.

Findlay S. 1995. Importance of surface-subsurface exchange in stream ecosystems: the hyporheic zone. *Limnology and Oceanography* **40**: 159–164. https://doi.org/10.4319/lo.1995.40.1.0159.

Fryirs KA, Brierley GJ. 2016. Assessing the geomorphic recovery potential of rivers: forecasting future trajectories of adjustment for use in management: assessing the geomorphic recovery potential of rivers. *Wiley Interdisciplinary Reviews: Water* **3**: 727–748. https://doi.org/10.1002/wat2.1158.

Gomez-Valez JD, Harvey JW, Cardenas MB, Kiel B. 2015. Denitrification in the Mississippi River network controlled by flow through river bedforms. *Nature Geoscience* **8**: 941–945. https://doi.org/10.1038/NGEO2567.

Gowan C, Fausch KD. 1996. Long-term demographic responses of trout populations to habitat manipulation in six Colorado streams. *Ecological Applications* **6**: 931–946. https://doi.org/10.2307/2269496.

Grimsley KJ, Rathburn SL, Friedman JM, Mangano JF. 2016. Debris flow occurrence and sediment persistence, Upper Colorado River Valley, CO. *Environmental Management* DOI: https://doi.org/10.1007/s00267-016-0695-1 [online] Available from Accessed 18 May 2016.http://link.springer.com/10.1007/s00267-016-0695-1

Harman CJ, Ward AS, Ball A. 2016. How does reach-scale stream-hyporheic transport vary with discharge? Insights from rSAS analysis of sequential tracer injections in a headwater mountain stream. *Water Resources Research* DOI: https://doi.org/10.1002/2016WR018832 [online] Available from: http://doi.wiley.com/10.1002/2016WR018832 (Accessed 20 October 2016)

Harvey JW, Bencala KE. 1993. The effect of streambed topography on surface-subsurface water exchange in mountain catchments. *Water Resources Research* **29**: 89–98.

Hauer FR, Locke H, Dreitz VJ, Hebblewhite M, Lowe WH, Muhlfeld CC, Nelson CR, Proctor MF, Rood SB. 2016. Gravel-bed river floodplains are the ecological nexus of glaciated mountain landscapes. *Science Advances* **2**: 13. https://doi.org/10.1126/sciadv.1600026.

Jefferson A, Clinton S, Osypian M. 2013. Transient storage versus hyporheic exchange in low-gradient headwater streams. Presented at the AGU Annual Meeting, San Francisco, CA.

Johnson TC, Slater LD, Ntarlagiannis D, Day-Lewis FD, Elwaseif M. 2012. Monitoring groundwater-surface water interaction using time-series and time-frequency analysis of transient three-dimensional electrical resistivity changes. *Water Resources Research* **48** W07506. DOI: https://doi.org/10.1029/2012WR011893.

Junk WJ, Bayley PB, Sparks RE. 1989. The flood pulse concept in river-floodplain system. *Proceedings of the International Large River Symposium*: 110–127. https://doi.org/10.1371/journal.pone.0028909.

Kondolf GM, Boulton AJ, O'Daniel S, Poole GC, Rahel FJ, Stanley EH, Wohl E, Bång A, Carlstrom J, Cristoni C, Huber H, Koljonen S, Louhi P, Nakamura K. 2006. Process-based ecological river restoration: visualizing three-dimensional connectivity and dynamic vectors to recover lost linkages. *Ecology and Society* **11**: 5.

Lake PS, Bond N, Reich P. 2007. Linking ecological theory with stream restoration. *Freshwater Biology* **52**: 597–615. https://doi.org/10.1111/j.1365-2427.2006.01709.x.

Menichino GT, Hester ET. 2014. Hydraulic and thermal effects of in-stream structure-induced hyporheic exchange across a range of hydraulic conductivities. *Water Resources Research* **50**: 4643–4661. https://doi.org/10.1002/2013WR014758.

Newbury R. 1995. Rivers and the art of stream restoration. Natural and Anthropogenic Influences in Fluvial Geomorphology. Geophysical Monograph 89 [online] Available from: http://www.cpp.edu/~marshall/rs414/RS414_Readings/Newbury_95_Art_of_Stream_Restor.pdf (Accessed 2 June 2017)

Nimmer RE, Osiensky JL, Binley AM, Williams BC. 2008. Three-dimensional effects causing artifacts in two-dimensional, cross-borehole, electrical imaging. *Journal of Hydrology* **359**: 59–70. https://doi.org/10.1016/j.jhydrol.2008.06.022.

NRCS U. 2016. Phantom Valley (688) - Site Information and Reports.

Palmer MA, Bernhardt ES, Allan JD, Lake PS, Alexander G, Brooks S, Carr J, Clayton S, Dahm CN, Follstad Shah J, Galat DL, Loss SG, Goodwin P, Hart DD, Hassett B, Jenkinson R, Kondolf GM, Lave R, Meyer JL, O'Donnell TK, Pagano L, Sudduth E. 2005. Standards for ecologically successful river restoration. *Journal of Applied Ecology* **42**: 208–217. https://doi.org/10.1111/j.1365-2664.2005.01004.x.

Rathburn SL, Rubin ZK, Wohl EE. 2013. Evaluating channel response to an extreme sedimentation event in the context of historical range of variability: upper Colorado River, USA. *Earth Surface Processes and Landforms* **38**: 391–406. https://doi.org/10.1002/esp.3329.

Rathburn SL, Shahverdian SM, Ryan SE. 2018. Post-disturbance sediment recovery: implications for watershed resilience. *Geomorphology*. https://doi.org/10.1016/j.geomorph.2017.08.039.

RMNP. 2013. EIS *Grand Ditch Breach Restoration*. National Park Service.

Rood SB, Braatne JH, Hughes FM. 2003. Ecophysiology of riparian cottonwoods: stream flow dependency, water relations and restoration. *Tree Physiology* **23**: 1113–1124.

Rubin Z, Rathburn SL, Wohl E, Harry DL. 2012. Historic range of variability in geomorphic processes as a context for restoration: Rocky Mountain National Park, Colorado, USA. *Earth Surface Processes and Landforms* **37**: 209–222. https://doi.org/10.1002/Esp.2249.

Runkel RL. 2015. On the use of rhodamine WT for the characterization of stream hydrodynamics and transient storage. *Water Resources Research* **51**: 6125–6142. https://doi.org/10.1002/2015WR017201.

Stanford JA, Ward JV. 1988. The hyporheic habitat of river ecosystems. *Nature* **335**: 64–66.

Tockner K, Malard F, Ward JV. 2000. An extension of the flood pulse concept. *Hydrological Processes* **14**: 2861–2883.

Toran L, Hughes B, Nyquist J, Ryan R. 2012. Using hydrogeophysics to monitor change in hyporheic flow around stream restoration structures. *Environmental and Engineering Geoscience* **18**: 83–97. https://doi.org/10.2113/gseegeosci.18.1.83.

Triska FJ, Kennedy VC, Avanzino RJ, Zellweger GW, Bencala KE. 1989. Retention and transport of nutrients in a third-order stream in northwestern California: hyporheic processes. *Ecology* **70**: 1893–1905. https://doi.org/10.2307/1938120.

Valett HM, Morrice JA, Dahm CN. 1996. Parent lithology, surface-groundwater exchange, and nitrate retention in headwater streams. *Limnology and Oceanography* **41**(2): 333–345.

Ward AS, Gooseff MN, Fitzgerald M, Voltz TJ, Singha K. 2014. Spatially distributed characterization of hyporheic solute transport during baseflow recession in a headwater mountain stream using electrical

geophysical imaging. *Journal of Hydrology* **517**: 362–377. https://doi.org/10.1016/j.jhydrol.2014.05.036.

Ward AS, Gooseff MN, Singha K. 2010a. Characterizing hyporheic transport processes- Interpretation of electrical geophysical data in coupled stream-hyporheic zone systems during solute tracer studies. *Advances in Water Resources* **33**: 1320–1330. https://doi.org/10.1016/j.advwatres.2010.05.008.

Ward AS, Singha K, Gooseff MN. 2010b. Imaging hyporheic zone solute transport using electrical resistivity. *Hydrological Processes* **24**: 948–953. https://doi.org/10.1002/hyp.7672.

Ward SH. 1990. Resistivity and induced polarization methods. In *Geotechnical and Environmental Geophysics*. Society of Exploration Geophysics: Anacortes, Washington US; 147–189.

Wegener P, Covino T, Wohl E. 2017. Beaver-mediated lateral hydrologic connectivity, fluvial carbon and nutrient flux, and aquatic ecosystem metabolism. *Water Resources Research* **53**(6): 4606–4623. https://doi.org/10.1002/2016WR019790.

Wohl E, Lane SN, Wilcox AC. 2015. The science and practice of river restoration. *Water Resources Research* **51**: 5974–5997. https://doi.org/10.1002/2014WR016874.

Wondzell SM. 2006. Effect of morphology and discharge on hyporheic exchange flows in two small streams in the Cascade Mountains of Oregon, USA. *Hydrological Processes* **20**: 267–287. https://doi.org/10.1002/hyp.5902.

Wyatt KH, Hauer FR, Pessoney GF. 2008. Benthic algal response to hyporheic-surface water exchange in an alluvial river. *Hydrobiologia* **607**: 151–161. https://doi.org/10.1007/s10750-008-9385-1.

Zedler JB. 2004. Compensating for wetland losses in the United States. *Ibis* **146**: 92–100.

Zedler JB, Kercher S. 2005. Wetland resources: status, trends, ecosystem services, and restorability. *Annual Review of Environment and Resources* **30**: 39–74. https://doi.org/10.1146/annurev.energy.30.050504.144248.

Supporting Information

Additional supporting information may be found online in the Supporting Information section at the end of the article.

Table S1: Stage/flow measurements used to compute hydraulic parameters for the Upstream and Downstream monitoring sites. The maximum 15-minute stage is included along with associated extrapolated discharge values. The percentage of flows extrapolated beyond the bankfull stage are included for each site in each year. Note: Upstream discharges on 2 July 2015 and 6 September 2015 were computed from hydraulic parameters and not directly measured, as indicated in the table with an asterisk.